Infrared absorption of gaseous c -ClCOOH and t -ClCOOH recorded with a step-scan Fourier-transform spectrometer

Li-Kang Chu and Yuan-Pern Lee

Citation: The Journal of Chemical Physics **130**, 174304 (2009); doi: 10.1063/1.3122722
View online: http://dx.doi.org/10.1063/1.3122722
View Table of Contents: http://scitation.aip.org/content/aip/journal/jcp/130/17?ver=pdfcov
Published by the AIP Publishing

Infrared absorption of gaseous *c*-ClCOOH and *t*-ClCOOH recorded with a step-scan Fourier-transform spectrometer

Li-Kang Chu[1] and Yuan-Pern Lee[2,a)]
[1]*Department of Applied Chemistry, National Chiao Tung University, Hsinchu 30010, Taiwan*
[2]*Department of Applied Chemistry and Institute of Molecular Science, National Chiao Tung University, Hsinchu 30010, Taiwan and Institute of Atomic and Molecular Sciences, Academia Sinica, Taipei 10617, Taiwan*

(Received 19 February 2009; accepted 31 March 2009; published online 4 May 2009)

Two conformers of ClCOOH were produced upon irradiation at 355 nm of a gaseous flowing mixture of Cl_2, HCOOH, and N_2. A step-scan Fourier-transform infrared spectrometer coupled with a multipass absorption cell was utilized to monitor the transient spectra of ClCOOH. Absorption bands with origins at 1808.0 and 1328.5 cm^{-1} are attributed to the C=O stretching and COH bending modes of *t*-ClCOOH, respectively; those at 1883.0 and 1284.9 cm^{-1} are assigned as the C=O stretching and COH bending modes of *c*-ClCOOH, respectively. These observed vibrational wavenumbers agree with corresponding values for *t*-ClCOOH and *c*-ClCOOH predicted with B3LYP/aug-cc-pVTZ density-functional theory and the observed rotational contours agree satisfactorily with simulated bands based on predicted rotational parameters. The observed relative intensities indicate that *t*-ClCOOH is more stable than *c*-ClCOOH by ~3 kJ mol^{-1}. A simple kinetic model is employed to account for the production and decay of ClCOOH. © *2009 American Institute of Physics*. [DOI: 10.1063/1.3122722]

I. INTRODUCTION

The hydrocarboxyl radical (HOCO) is an important intermediate in the reaction of OH with CO, which is the major reaction responsible for the oxidation of CO to CO_2 in the atmosphere and in combustion systems.[1–4] HOCO is also produced in other reactions. The reaction of OH with formic acid (HCOOH), the most abundant carboxylic acid in the troposphere,[5] is not only a source of HOCO but also a major sink for HCOOH.[6] Another important source of HOCO in the atmosphere is the reaction of Cl with HCOOH. In the laboratory, this reaction also serves as a source to produce HOCO.[7]

West and Rollefson reported that CO_2 and HCl were produced upon irradiation of a mixture of Cl_2 and HCOOH; they proposed that HOCO and ClCOOH are reaction intermediates.[8] Li *et al.* irradiated mixtures of Cl_2, O_2, HCOOH, and He with a Xe flash lamp to investigate the bimolecular rate coefficients of reactions (2) and (4) based on the following mechanism:

$$Cl_2 + h\nu \rightarrow 2Cl \quad (1)$$

$$Cl + HCOOH \rightarrow HCl + HOCO \quad (2)$$

$$HOCO + O_2 \rightarrow CO_2 + HO_2 \quad (3)$$

$$Cl + HOCO \rightarrow HCl + CO_2. \quad (4)$$

Values of $k_2=(1.83\pm0.12)\times10^{-13}$ and $k_4=(4.8\pm1.0)\times10^{-11}$ cm^3 $molecule^{-1}$ s^{-1} were derived on fitting the temporal profile of CO_2 probed with the P(4) line in the ν_3 band of CO_2 with a simplified equation of exponential rise and a literature value of $k_3=1.9\times10^{-12}$ cm^3 $molecule^{-1}$ s^{-1}.[9] By comparison of the decay rates of the reactant and a reference compound determined with infrared (IR) absorption, Wallington *et al.*[10] evaluated $k_2=(2.00\pm0.25)\times10^{-13}$ cm^3 $molecule^{-1}$ s^{-1} under 700 Torr of N_2 or synthetic air.

The experiment on reaction of Cl with monodeuterated formic acid HCOOD indicated that reaction (2) proceeds predominantly via abstraction of the H-atom on the carbon to form HOCO rather than abstraction of the hydroxyl hydrogen to form HCO_2.[7] This finding is consistent with the results of Tyndall *et al.*[11] who reported a yield of $96\pm5\%$ for CO_2 from the reaction of Cl with HCOOH in 700 Torr of air based on their measurements with Fourier-transform infrared (FTIR) spectra; CO_2 was presumably produced from reactions (3) and (4).

Li *et al.* proposed that reaction (4) might proceed via direct abstraction of a H-atom, formation of a ClCOOH complex, or a short-lived intermediate in which the C–Cl bond is rapidly formed and the H atom is rapidly abstracted.[9] In contrast, West and Rollefson postulated the formation of transient chloroformic acid (ClCOOH) that decomposes readily to HCl and CO_2 via the *cis* configuration (*c*-ClCOOH). For convenience, the *trans* and *cis* notations in this paper follow the same nomenclature as for HCOOH,[12] therefore *c*-ClCOOH has its H atom *cis* to the Cl atom with respect to the C–O bond.

Herr and Pimentel[13] photolyzed a mixture of Cl_2 and HCOOH with a flash lamp and monitored reaction intermediates with a rapid-scan IR spectrometer; a transient band at

a)Author to whom correspondence should be addressed. Electronic mail: yplee@mail.nctu.edu.tw. FAX: 886-3-5713491.

768 cm^{-1} was observed and assigned as the C–Cl stretching mode of ClCOOH. Jensen and Pimentel[14] further studied the unimolecular decomposition

$$ClCOOH \rightarrow HCl + CO_2 \quad (5)$$

over the temperature range 288–343 K by monitoring the decay of this 768 cm^{-1} band and derived a rate coefficient of $k_5 = 5 \times 10^{13} \exp(-7050/T)$ s^{-1}. They proposed that the rate-determining step for reaction (5) is the conversion from *t*-ClCOOH to *c*-ClCOOH with a barrier about 58 ± 7 kJ mol^{-1}. No distinction of absorption between conformers of ClCOOH was discussed, nor was any other IR absorption band of ClCOOH reported.

Several quantum-chemical calculations on *c*-ClCOOH and *t*-ClCOOH have been performed.[15–19] The conformation notation employed in this paper is consistent with that used in Refs. 17 and 18, but is the reverse of that in Refs. 14–16 and 19. Conformer *t*-ClCOOH is predicted to be more stable than *c*-ClCOOH by 4–11 kJ mol^{-1} and the barrier to convert from *trans* to *cis* conformers is 41–50 kJ mol^{-1}, depending on the methods of calculation.[15,17,19] Stephenson *et al.*[17] argued that because of the disagreement between the vibrational wavenumber (768 cm^{-1}) of the only band observed by Pimentel and coworkers[13,14] and the value (725 cm^{-1}) predicted quantum chemically, a search for the carbonyl absorption in the 1800–1880 cm^{-1} region would provide crucial evidence whether ClCOOH was indeed observed previously.

We have demonstrated that by coupling a multipass absorption cell with a step-scan FTIR spectrometer, time-resolved IR absorption spectra of transient intermediates in gaseous reactions can be recorded.[20–25] Here such an application is further demonstrated by our observation of transient IR absorption spectra of *c*-ClCOOH and *t*-ClCOOH upon photolysis of a gaseous mixture of $Cl_2/HCOOH/N_2$ at 363 K.

II. EXPERIMENTS

The sample compartment of a step-scan Fourier-transform spectrometer (Thermo Nicolet, Nexus 870) contains a flow reactor inside which a set of White cell mirrors with a base path length of 20 cm and an effective path length of 6.4 m was installed.[21,22] The flow reactor has a volume of ~1.6 L and accommodates two rectangular quartz windows (3×12 cm^2) to pass the photolysis beam that propagates perpendicularly to multiply passed IR beams. The beam from a frequency-tripled Nd:YAG (yttrium aluminum garnet) laser (LOTIS TII, LS-2137/20, 11 Hz, 74 mJ $pulse^{-1}$, beam dimension 0.5 cm^2) emitting at 355 nm passed through these quartz windows and was reflected eight times with a pair of external laser mirrors to photodissociate a flowing mixture of $Cl_2/HCOOH/N_2$. We obtained temporally resolved difference absorption spectra from interferograms recorded simultaneously with ac- and dc-coupled signals of a mercury cadmium telluride detector (20 MHz response bandwidth).[21,26] The ac-coupled signal was further amplified (Stanford Research Systems, Model SR560, bandwidth 100 Hz–1 MHz) 20 times before being transferred to an external 14-bit digitizer (Gage Applied Technology, CompuScope 14100, 10^8 sample s^{-1}), whereas the dc-coupled signal was sent directly to the internal 16-bit digitizer (2×10^5 sample s^{-1}) of the spectrometer. Typically, 500 data points were acquired at 1 μs integrated intervals (100 dwells at 10 ns gate width) to cover a period of 500 μs after photolysis; these signals were typically averaged over 40 laser shots at each scan step. With appropriate optical filters to define a narrow spectral region, we performed undersampling to decrease the size of the interferogram, hence the duration of data acquisition. For spectra in the range 1055–2100 cm^{-1}, 1192 scan steps at a resolution of 2.0 cm^{-1} were completed within ~1.5 h. For spectra in the range 1000–3150 cm^{-1} at a resolution of 5.0 cm^{-1}, 1472 scan steps were completed within ~2 h.

Experimental conditions were as follows: flow rates $F_{HCOOH} \cong 0.25-1.05$, $F_{Cl_2} \cong 2.1$, and $F_{N_2} \cong 26.1$ STP cm^3 s^{-1} (STP denotes standard temperature 273.15 K and pressure 1 atm); total pressure ≅ 58 Torr. To minimize the formation of dimeric formic acid, the flow reactor was heated to $T = 363$ K with heated water circulated from a thermostat bath through the jacket of the reactor. Based on the equilibrium constant between monomeric and dimeric HCOOH, the fraction of $(HCOOH)_2$ is less than 10% under our experimental conditions.[27]

The efficiency of photolysis of Cl_2 is estimated to be ~4% based on the absorption cross section of $\sim 1.6 \times 10^{-19}$ cm^2 $molecule^{-1}$ at 355 nm (Ref. 28) and the laser fluence of $\sim 2.6 \times 10^{17}$ photons cm^{-2}. HCOOH (99%, Riedel-de Haën), Cl_2 (99.99%, AGA Specialty Gases), and N_2 (99.995%, AGA Specialty Gases) were used without further purification.

III. QUANTUM-CHEMICAL CALCULATIONS

The equilibrium geometry, vibrational wavenumbers, and IR intensities of *c*-HCOOH, *t*-HCOOH, *c*-HOCO, *t*-HOCO, *c*-ClCOOH, and *t*-ClCOOH were calculated with the B3LYP density-functional theory using the GAUSSIAN 03 program.[29] The B3LYP method uses Becke's[30] three-parameter hybrid exchange functional with a correlation functional of Lee *et al.*[31] Dunning's correlation-consistent polarized-valence triple-zeta basis set, augmented with *s*, *p*, *d*, and *f* functions (aug-cc-pVTZ) was applied in these calculations.[32,33] Analytic first derivatives were utilized in geometry optimization, and vibrational wavenumbers were calculated analytically at each stationary point. Rotational parameters of *c*-HOCO, *t*-HOCO, *c*-ClCOOH, and *t*-ClCOOH in their vibrational ground and excited ($v_i = 1$) states were also calculated with B3LYP/aug-cc-pVTZ for spectral simulation.

IV. RESULTS

A. Absorption spectra recorded upon photolysis of a mixture of $HCOOH/Cl_2/N_2$

The absorption spectrum of a static gaseous mixture of $HCOOH/Cl_2/N_2$ (1/0.6/10.7 at 54.3 Torr) at 363 K was recorded with a conventional FTIR technique. The characteristic bands of *t*-HCOOH at 2943, 2196, 1770, 1387, 1229, and 1105 cm^{-1} are consistent with literature values.[34] Upon

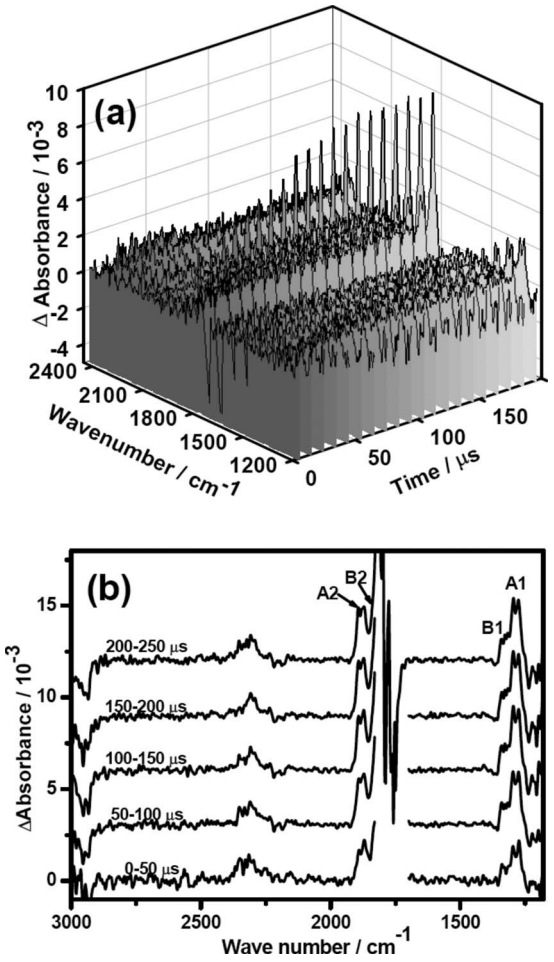

FIG. 1. (a) Three-dimensional plot of time-resolved difference absorption spectra upon laser photolysis (355 nm, 11 Hz, 74 mJ cm^{-2}) of a flowing mixture of $HCOOH/Cl_2/N_2$ (1/9/103 at 58 Torr) at 363K; spectral resolution 5.0 cm^{-1}. (b) Spectra integrated over 50 μs intervals: downward features are due to consumption of HCOOH (the saturation near 1750 cm^{-1} is truncated), whereas upward features A1 and A2 correspond to formation of *c*-ClCOOH and features B1 and B2 correspond to formation of *t*-ClCOOH. The band near 2350 cm^{-1} is due to CO_2.

irradiation of this mixture with laser emission at 355 nm (70 mJ $pulse^{-1}$, 10 Hz for 1 min), an intense broad band of CO_2 near 2349 cm^{-1} and a rotational progression of HCl with an origin at 2885 cm^{-1} were observed, consistent with previous results.[9,11] No absorption bands can be assigned to HOCO or ClCOOH in these static cell experiments.

The temporally and spectrally resolved difference spectra recorded upon irradiation of a flowing mixture of $HCOOH/Cl_2/N_2$ (1/9/103 at 58 Torr and 363 K) with the step-scan FTIR spectrometer are shown in Fig. 1(a) as a three-dimensional plot. The consumption of HCOOH shown as downward features near 1750 cm^{-1} is partially truncated due to saturation of the parent absorption. Several features near 1850 and 1300 cm^{-1} were observed to increase with time. Spectra integrated at 50-μs intervals are shown in Fig. 1(b). In addition to the downward peaks near 2943, 2196, 1770, and 1229 cm^{-1} due to destruction of HCOOH, the CO_2 band near the 2350 cm^{-1} region and four bands near 1285, 1883, 1329, and 1808 cm^{-1}, labeled as A1, A2, B1, and B2 respectively, gradually increased in intensity and attained their maximal absorbance near 100–150 μs. These four new bands diminished in intensity afterward and became nearly undetectable ~500 μs after laser irradiation.

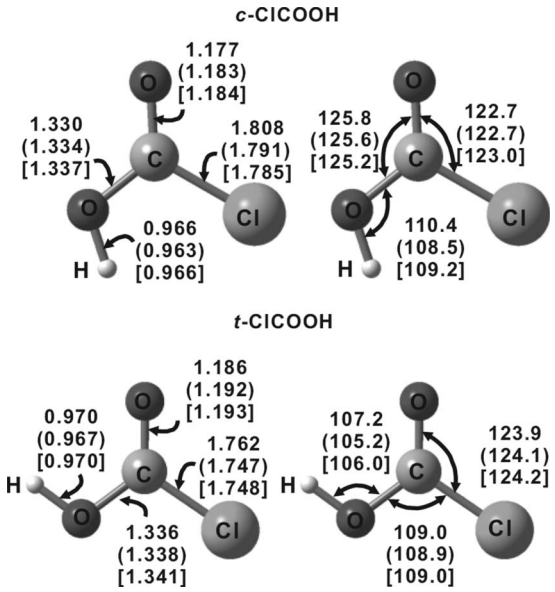

FIG. 2. Geometries predicted with the B3LYP/aug-cc-pVTZ method for *c*-ClCOOH and *t*-ClCOOH. Bond lengths are in Å and bond angles in degrees. The values in parentheses are derived with MP2//6-311G** (Ref. 17) and the values in brackets are derived with CCSD(T)/cc-pVTZ (Ref. 19).

B. Quantum-chemical calculations

Geometries of *c*-ClCOOH and *t*-ClCOOH predicted with B3LYP/aug-cc-pVTZ are shown in Fig. 2. For comparison, results from MP2/6-311G** (Ref. 17) and CCSD(T)/aug-cc-pVTZ (Ref. 19) are listed in parentheses and brackets, respectively; the deviations among these results are within 2% for both conformers.

The conformer *t*-ClCOOH is more stable than *c*-ClCOOH; the zero-point-energy corrected energy of *t*-ClCOOH is smaller than *c*-ClCOOH by 2 kJ mol^{-1} at the B3LYP/aug-cc-pVTZ level of theory, slightly smaller than values ~8 kJ mol^{-1} reported by Francisco and Ghoul[15] using the UMP2/6-311G** method and by Stephenson *et al.*[17] using MP2/6-311G**, but similar to a value of 4 kJ mol^{-1} reported by Yu *et al.*[19] using the high-level CCSD(T)/aug-cc-pVTZ method.

The isomerization barrier from *t*-ClCOOH to *c*-ClCOOH was calculated to be 41–50 kJ mol^{-1} using various methods,[15,17,19] as compared to the experimental value of 58 ± 7 kJ mol^{-1} determined by Jensen and Pimentel[14] from the temperature dependence of the decay of the 768 cm^{-1} band assigned to ClCOOH; they assumed that the rate-determining step is the *trans-cis* isomerization of ClCOOH before its rapid decomposition to HCl and CO_2.

The harmonic vibrational wavenumbers and IR intensities of *t*-ClCOOH and *c*-ClCOOH predicted with the B3LYP/aug-cc-pVTZ method are listed in Table I. Values predicted previously with MP2/6-311G** (Ref. 17) and HF/3-21G (Ref. 15), including the fundamental ($v=0 \rightarrow v=1$) vibrational wavenumbers reported for *t*-ClCOOH,[17] are listed also for comparison. For *t*-ClCOOH, the most intense absorption bands are predicted to be at 1844, 1127, and 706 cm^{-1}, cor-

TABLE I. Comparison of harmonic vibrational wavenumbers (cm^{-1}) and IR intensities (listed in parentheses in km mol^{-1}) of *c*-ClCOOH and *t*-ClCOOH derived from experiments and calculations.

ν_i	Mode	B3LYP /aug-cc-pVTZ	MP2 /6-311G**	MP2 fundamental	HF /3-21G	Gas
			t-ClCOOH			
ν_1	O–H stretch	3724 (92)	3819 (100)	3633	3829	
ν_2	C=O stretch	1844 (464)	1879 (399)	1840	1998	1808.0 (B2)
ν_3	COH bend	1332 (63)	1368 (65)	1346	1438	1328.5 (B1)
ν_4	C–O stretch	1127 (366)	1167 (406)	1139	1174	
ν_5	OCO bend/C–Cl stretch	706 (157)	733 (162)	725	728	768?[a]
ν_6	ClCOO out-of-plane	705 (48)	714 (62)	690	709	
ν_7	ClCOH torsion	549 (82)	576 (85)	552	544	
ν_8	OCO bend/C–Cl stretch	480 (5)	505 (4)	497	479	
ν_9	ClCO bend	409 (2)	423 (1)	417	404	
			c-ClCOOH			
ν_1	O–H stretch	3775 (88)	3877 (108)		3903	
ν_2	C=O stretch	1919 (429)	1944 (369)		2108	1883.0 (A2)
ν_3	COH bend	1286 (407)	1304 (430)		1321	1284.9 (A1)
ν_4	C–O stretch	1131 (167)	1157 (171)		1205	
ν_5	OCO bend/C–Cl stretch	691 (114)	706 (131)		698	
ν_6	ClCOO out-of-plane	679 (3)	686 (4)		695	
ν_7	ClCOH torsion	519 (108)	485 (139)		454	
ν_8	OCO bend/C–Cl stretch	452 (22)	473 (18)		437	
ν_9	ClCO bend	402 (8)	415 (10)		392	
References		This work	17	17	15	This work

[a]References 13 and 14.

responding approximately to C=O stretching, C–O stretching, and the C–Cl stretching mixed with OCO bending modes, respectively. Intense absorption bands of *c*-ClCOOH are predicted to occur at 1919, 1286, and 1131 cm^{-1}, attributable to C=O stretching, COH bending, and C–O stretching modes, respectively. The values predicted for *t*-ClCOOH are within 5.2% of the harmonic wavenumbers and 3.5% of the fundamental vibrational wavenumbers predicted previously with MP2/6-311G**.[17] Similarly, the values predicted for *c*-ClCOOH are within 7.0% of the harmonic wavenumbers predicted previously with MP2/6-311G**.[17]

The predicted molecular axes, vibrational displacements (thin arrows), and their corresponding dipole derivatives (thick dashed arrows) for the C=O stretching and COH bending modes of *c*-ClCOOH and *t*-ClCOOH are shown in Fig. 3. The projection vectors of the dipole derivative onto the molecular axes represent the weighting of the transition types. The C=O stretching band of *t*-ClCOOH is a hybrid type with a ratio of *a*-type/*b*-type=1/2, whereas the COH bending band of *t*-ClCOOH is a hybrid type with a ratio of *a*-type/*b*-type=3/1. For *c*-ClCOOH, the C=O stretching band has a ratio of *a*-type/*b*-type=43/57, whereas the COH bending band has a ratio of *a*-type/*b*-type=1/1.

Rotational parameters for the equilibrium geometry, the vibrational ground state, and excited states (v_i=1) of each vibrational mode of *c*-ClCOOH and *t*-ClCOOH were calculated with the B3LYP/aug-cc-pVTZ method. These parameters and the ratios of A'/A'', B'/B'', and C'/C'', in which the prime and double prime indicate the excited and ground states, respectively, for the C=O stretching and COH bending modes of these two conformers of ClCOOH are listed in Table II.

The HOCO radical has been well characterized with quantum-chemical calculations.[35–42] We performed calculations on HOCO at the same level as for ClCOOH mainly for comparison purposes. Vibrational wavenumbers (in cm^{-1}) and IR intensities (in km mol^{-1}) for *c*-HOCO are 3562 (16),

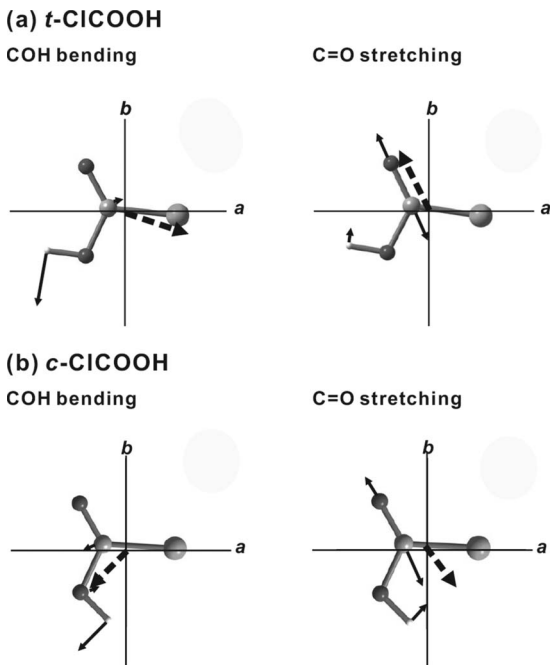

FIG. 3. Displacement vectors (thin solid arrows) and vectors of dipole derivatives (thick dashed arrows) predicted with the B3LYP/aug-cc-pVTZ method for the COH bending and C=O stretching modes of (a) *t*-ClCOOH and (b) *c*-ClCOOH. Molecular axes *a* and *b* are shown in the plane; the axis *c* points out of the plane perpendicularly.

TABLE II. Comparison of rotational parameters of *c*-ClCOOH and *t*-ClCOOH in ground and vibrationally excited states predicted with B3LYP/aug-cc-pVTZ.

	Equilibrium	$v=0$	$v=1$	$v=1/v=0$
		t-ClCOOH		
		C=O stretch		
A/cm^{-1}	0.401 508	0.398 943	0.397 499	$A'/A''=0.9964$
B/cm^{-1}	0.171 810	0.171 132	0.170 964	$B'/B''=0.9990$
C/cm^{-1}	0.120 322	0.119 605	0.119 412	$C'/C''=0.9984$
		COH bend		
A/cm^{-1}	0.401 508	0.398 943	0.398 600	$A'/A''=0.9991$
B/cm^{-1}	0.171 810	0.171 132	0.171 151	$B'/B''=1.0001$
C/cm^{-1}	0.120 322	0.119 605	0.119 469	$C'/C''=0.9989$
		c-ClCOOH		
		C=O stretch		
A/cm^{-1}	0.390 067	0.387 953	0.386 525	$A'/A''=0.9963$
B/cm^{-1}	0.170 474	0.169 698	0.169 697	$B'/B''=1.0000$
C/cm^{-1}	0.118 628	0.117 908	0.117 785	$C'/C''=0.9990$
		COH bend		
A/cm^{-1}	0.390 067	0.387 953	0.387 793	$A'/A''=0.9996$
B/cm^{-1}	0.170 474	0.169 698	0.169 617	$B'/B''=0.9995$
C/cm^{-1}	0.118 628	0.117 908	0.117 747	$C'/C''=0.9986$

1860 (339), 1293 (1), 1067 (165), 598 (31), and 588 (105); corresponding values for *t*-HOCO are 3786 (125), 1897 (246), 1239 (238), 1079 (79), 620 (4), and 550 (85). For *c*-HOCO, the most intense absorption bands are at 1860 and 1067 cm^{-1}, corresponding approximately to the C=O stretching and C–O stretching modes, respectively, whereas the most intense bands of *t*-HOCO are at 1897 and 1239 cm^{-1}, corresponding to the C=O stretching and COH bending modes, respectively. The COH bending mode of *c*-HOCO at 1293 cm^{-1} has a very small intensity, as indicated above.

V. DISCUSSION

A. Assignments of *c*-ClCOOH and *t*-ClCOOH

At 363 K, negligible dimeric formic acid is present; therefore only the reactions of Cl atom with HCOOH need to be considered. Based on theoretical calculations, the reaction might involve two reaction intermediates, HOCO and ClCOOH.[19] The ν_1 ($\sim$3636 cm^{-1}) and ν_2 bands ($\sim$1853 cm^{-1}) of gaseous *t*-HOCO have been characterized previously.[43–45] Most vibrational bands of *t*-HOCO isolated in CO,[46] Ar,[47] Ne matrices,[48] and *c*-HOCO isolated in a CO matrix have been reported.[46] Only one band, the C–Cl stretching (ν_5) mode near 768 cm^{-1}, of gaseous ClCOOH (presumably due to *trans* configuration) was reported.[13,14]

Upon excitation of a flowing mixture of $HCOOH/Cl_2/N_2$, four transient bands near 1285, 1883, 1329, and 1808 cm^{-1}, showed as A1, A2, B1, and B2 in Fig. 1(b), were observed. Bands A1 and A2 correlate well in intensity under various experimental conditions; bands B1 and B2 also correlate with each other, even though we cannot positively rule out the possibility that other combinations of these features are correlated.

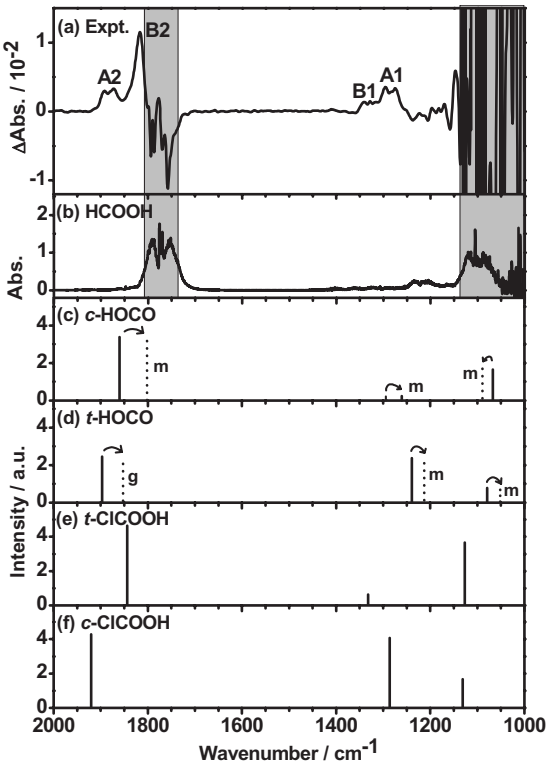

FIG. 4. (a) Transient difference absorption spectrum recorded upon photolysis at 355 nm of a flowing mixture of $HCOOH/Cl_2/N_2$ (1/9/103 at 58 Torr) at 363 K; resolution is 5.0 cm^{-1} and averaging period is 100–150 μs. (b) Absorption of HCOOH with the saturated spectral regions indicated with grey color. [(c)–(f)] Stick spectra of *c*-HOCO, *t*-HOCO, *t*-ClCOOH, and *c*-ClCOOH, respectively, based on harmonic vibrational wave numbers and IR intensities predicted with the B3LYP/aug-cc-pVTZ method. Experimental values of HOCO are also shown as arrows [*m* for matrix isolation (Refs. 46–48) and *g* for gas phase (Ref. 44)].

The possibility that these bands are due to *t*-HOCO is eliminated because the C=O stretching band of *t*-HOCO reported by Sears *et al.*[44] lies at 1852.567 cm^{-1}, at least 32 cm^{-1} separated from the observed bands. Furthermore, the ν_3 mode of *t*-HOCO isolated in Ar or Ne was observed to absorb at $\sim$1210 cm^{-1},[47,48] 74 cm^{-1} from the observed A1 band.

According to the only report on IR absorption of *c*-HOCO, an intense band at 1797 cm^{-1} and a weaker one at 1261 cm^{-1} were assigned to absorption of the C=O stretching and COH bending modes of *c*-HOCO isolated in solid CO.[46] Observed wavenumbers of the B2 (1808 cm^{-1}) and A1 (1285 cm^{-1}) bands in this work fit satisfactorily with these reported values. However, according to quantum-chemical calculations, two most intense absorption bands of *c*-HOCO are at 1860 and 1067 cm^{-1}, the latter corresponds to approximately the C–O stretching mode. The intensity of the COH bending mode (predicted to be 1293 cm^{-1} at B3LYP/aug-cc-pVTZ) has an IR intensity 1/340 that of the C=O stretching band predicted at 1860 cm^{-1}. Observed intensity ratio for these two bands disagrees with theoretical predictions.

In Fig. 4, the observed transient spectrum in the 1000–2000 cm^{-1} region is compared to unscaled harmonic vibrational wavenumbers of *c*-HOCO, *t*-HOCO, *c*-ClCOOH, and *t*-ClCOOH predicted with B3LYP/aug-cc-pVTZ; bands

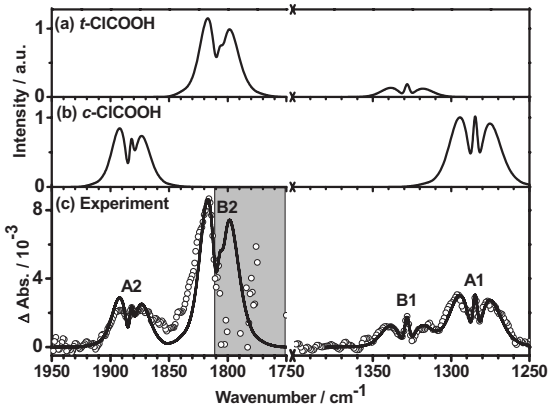

FIG. 5. Comparison of the observed and simulated spectra of ClCOOH in the region 1250–1950 cm^{-1}. (a) Simulated bands for the COH bending mode (ν_0=1328.5 cm^{-1} and *a*-type/*b*-type=3/1) and the C=O stretching mode (ν_0=1808.0 cm^{-1} and *a*-type/*b*-type=1/2) of *t*-ClCOOH. (b) Simulated bands for the COH bending mode (ν_0=1284.9 cm^{-1} and *a*-type/*b*-type=1/1) and the C=O stretching mode (ν_0=1883.0 cm^{-1} and *a*-type/*b*-type=43/57) of *c*-ClCOOH. (c) Simulated (in solid line) and observed spectra (open circles) 100–300 μs upon irradiation of a flowing mixture of $HCOOH/Cl_2/N_2$ (1/2.1/24.6 at 58.1 Torr) at 363 K; spectral resolution 2.0 cm^{-1}. See text.

previously observed for *c*-HOCO and *t*-HOCO are also indicated with dashed lines and marked with *m* for matrix and *g* for gaseous experiments. The spectrum of HCOOH is also shown in Fig. 4(b) to indicate the regions (1730−1810 and 1000–1140 cm^{-1}, with gray color) that are unusable because of saturated absorption of the parent. If we assume small corrections to derive expected vibrational wavenumbers from calculated harmonic vibrational wavenumbers of ClCOOH, similar to those indicated in frames (c) and (d) of Fig. 4 for HOCO, the expected vibrational wavenumbers and relative IR intensities of *t*-ClCOOH and *c*-ClCOOH (Table I) fit well with observed (B1, B2) and (A1, A2) groups of bands, respectively. If bands A1 and A2 are assigned to the COH bending and C=O stretching modes of *c*-ClCOOH, the experimental values deviate only about 2% and 3%, respectively, from our calculated harmonic wavenumbers. Similarly, if bands B1 and B2 are attributed to the COH bending and C=O stretching modes of *t*-ClCOOH, the deviations are 2% and 1%, respectively.

As a derivation of rotational parameters from observed spectra is unlikely to be practicable with the present spectral resolution, we simulated the band contour using the molecular parameters predicted with B3LYP/aug-cc-pVTZ for comparison with observed spectra. With the SPECVIEW program[49] we simulated the spectrum of each band using predicted rotational parameters A', A'', B', B'', C', and C'' (Table II), J_{max}=120, T=363 K, and a Doppler width (full width at half maximum) of 2.0 cm^{-1}. The resultant rotational contours simulated for these four bands with *a*-type/*b*-type ratios calculated quantum chemically (Sec. IV B) are shown in frames (a) and (b) of Fig. 5 for *t*-ClCOOH and *c*-ClCOOH, respectively. A comparison of the observed transient spectrum averaged over 100–150 μs (with open circle marks) with the combined simulated contour (solid lines) of these four bands is shown in Fig. 5(c). The missing data for the P branch of the B2 band in the 1750–1810 cm^{-1} region are due to interference from saturated absorption of HCOOH. For this simulation, A1 band has ν_0=1284.9 cm^{-1} with *a*-type/*b*-type =1/1, A2 band has ν_0=1883.0 cm^{-1} with *a*-type/*b*-type =43/57, B1 band has ν_0=1328.5 cm^{-1} with *a*-type/*b*-type =3/1, and B2 band has ν_0=1808.0 cm^{-1} with *a*-type/*b*-type=1/2; values of ν_0 are listed in Table I for comparison with calculations. Observed integrated intensity ratios of C=O stretching to COH bending modes are ~6.5 and ~1.1, respectively, for *t*-ClCOOH and *c*-ClCOOH, which are consistent with the quantum-chemically predicted values of 7.2 and 1.1, respectively.

When the quantum-chemically predicted IR intensities are used, the population ratios of *t*-ClCOOH to *c*-ClCOOH can be estimated to be $\sim 2.5 \pm 0.3$ based on the observed integrated intensities of B1 and A1 bands; the error limits reflect errors only in simulation, not the errors in the predicted IR intensities. If we assume that the simulation of the B2 band is reliable even though only part of the band was observed, the observed population ratio is $\sim 2.6 \pm 0.3$ based on the integrated intensities of simulated B2 and A2 bands, consistent with the result derived from B1 and A1 bands. A concentration of *t*-ClCOOH greater than that of *c*-ClCOOH is consistent with the quantum-chemically predicted result that *t*-ClCOOH is slightly more stable than *c*-ClCOOH. Assuming a Boltzmann population at 363 K, we derive from the observed intensity ratio an energy difference of 2.8 ± 0.3 kJ mol^{-1} between these two configurations. If an error of a factor of 2 is assumed for the predicted IR intensity, then $\Delta E = 2.8 \pm 1.9$ kJ mol^{-1}. This value is consistent with values of 2 kJ mol^{-1} calculated with B3LYP/aug-cc-pVTZ in this work and 4 kJ mol^{-1} reported by Yu *et al.*[19] using the CCSD(T)/aug-cc-pVTZ method, but slightly smaller than values ~8 kJ mol^{-1} reported by Francisco and Ghoul[15] using UMP2/6-311G**, and by Stephenson *et al.*[17] using MP2/6-311G**; the latter two methods used a smaller basis set and are expected to be less accurate.

Considering possible chemical reactions, vibrational wavenumbers, rotational contours, relative IR intensities, and relative concentrations, we are confident of the assignments of the four transient features A1, A2, B1, and B2 observed near 1285, 1883, 1329, and 1808 cm^{-1} to the COH bending and C=O stretching modes of *c*-ClCOOH, COH bending, and C=O stretching modes of *t*-ClCOOH, respectively. According to quantum-chemical calculations, the C–Cl stretching (691 cm^{-1}) and C–O stretching (1131 cm^{-1}) modes of *c*-ClCOOH are expected to have intensities ~0.25 those of the A1 and A2 bands, and the C–Cl stretching (706 cm^{-1}) and C–O stretching (1127 cm^{-1}) modes of *t*-ClCOOH are expected to have intensities slightly smaller than that of the B2 bands. The C–Cl stretching mode is beyond our detection range (950–7000 cm^{-1}), whereas the C–O stretching mode of ClCOOH is severely overlapped by the intense absorption of HCOOH (Fig. 4). The 768 cm^{-1} band observed by Pimentel and coworkers[13,14] does not match the predicted wavenumber for the C–Cl stretching mode of *c*-ClCOOH or *t*-ClCOOH.

According to literature values, *t*-HOCO absorbs at 1852.6 (Ref. 44) and ~1210 cm^{-1}.[47,48] The 1852.6 cm^{-1} band might be buried between the B2 and A2 bands, but we

observed no discernible feature in the 1200–1250 cm^{-1} region near the A1 band. It is likely that *t*-HOCO was not produced directly from reaction (2) because *t*-HCOOH is the dominant conformer and the Cl atom only abstracts the hydrogen on the C atom. Conformer *c*-HOCO was observed only in a CO matrix,[46] with two intense lines at 1797 and 1088 cm^{-1}; the 1261 cm^{-1} line is expected to have a small intensity according to calculations with the B3LYP/aug-cc-pVTZ method. Both absorption regions (~1800 and 1090 cm^{-1}) for *c*-HOCO were inaccessible in this work because of the intense absorption of HCOOH.

B. Possible mechanism of the Cl+HCOOH reaction

The reaction of Cl with HCOOH is believed to proceed via reaction (2),

$$Cl + HCOOH \rightarrow HCl + HOCO. \quad (2)$$

Tyndall *et al.*[11] determined a yield of $96 \pm 5\%$ for CO_2 and suggested that the other channel

$$Cl + HCOOH \rightarrow HCl + HCO_2. \quad (6)$$

is unimportant. Miyoshi *et al.*[7] also showed that reaction (6) is unimportant by deuteration experiments. Yu *et al.*[50] employed UQCISD(T, full)/6-311++G(3*df*,2*p*)//UMP2(full)/6-311+G(*d*,*p*) and reported that reactions (2) and (6) have barriers of 3.7 and 68 kJ mol^{-1}, respectively. They concluded that the C-site hydrogen abstraction of *t*-HCOOH to form *c*-HOCO dominates, consistent with experimental observations. Rate coefficient $k_2 = (1.83 \pm 0.12) \times 10^{-13}$ cm^3 $molecule^{-1}$ s^{-1} near 298 K was reported by Li *et al.*,[9] similar to $k_2 = (2.00 \pm 0.25) \times 10^{-13}$ cm^3 $molecule^{-1}$ s^{-1} reported by Wallington *et al.*[10]

Further reaction of HOCO with Cl_2 is unimportant because this reaction is expected to have a large barrier. In contrast, reaction of Cl with HOCO to form HCl and CO_2 is expected to be rapid,

$$Cl + HOCO \rightarrow HCl + CO_2 \quad (4)$$

and the rate coefficient was determined to be $k_4 = (4.8 \pm 1.0) \times 10^{-11}$ cm^3 $molecule^{-1}$ s^{-1} near 298 K, ~250 times greater than k_2.[9] Yu *et al.*[19] employed CCSD(T) theory to investigate reaction (4) and found that the reaction occurs via a ClCOOH intermediate that is formed through the barrierless addition reaction of Cl to the carbon atom in HOCO. The ClCOOH intermediate dissociate into HCl and CO_2 through a four-center (Cl–C–O–H) transition state that lies ~234 kJ mol^{-1} below the asymptotic reactant channel. They derived a thermal rate coefficient of $k_4 = 3.0 \times 10^{-11}$ cm^3 $molecule^{-1}$ s^{-1}, consistent with experimental results. They also employed a direct MP2/6-31G(*d*) molecular dynamics method to find reactive trajectories of two kinds, both of which proceed through ClCOOH with lifetimes ~0.31 and 1.9 ps, respectively. They suggested that the long-lived ClCOOH might be stabilized with a third collision partner, consistent with our experimental observation of both conformers of ClCOOH upon photolysis of a mixture of Cl_2 and HCOOH under 58 Torr of N_2.

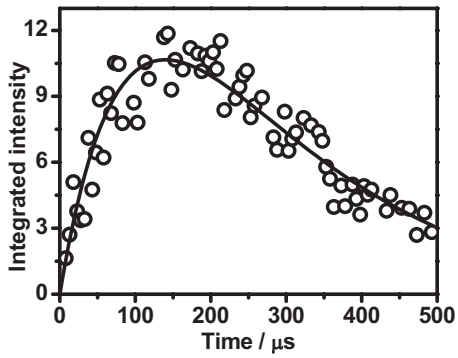

FIG. 6. Temporal profile of ClCOOH integrated over 1350–1250 cm^{-1} upon 355 nm photolysis of a flowing mixture of $HCOOH/Cl_2/N_2$ (1/9/103 at 58 Torr). Fitted results are represented with solid lines; see text.

We employ a simple mechanism to describe the reactions in our system,

$$Cl + HCOOH \rightarrow HCl + HOCO \quad (2)$$

$$Cl + HOCO \rightarrow ClCOOH \quad (7)$$

$$ClCOOH \rightarrow HCl + CO_2 \quad (5)$$

in which k_7 is expected to be much larger than k_2, as supported by reported values of $k_4 \gg k_2$; hence the rate-determining step for formation of ClCOOH is reaction (2). Under such conditions, [HOCO] is expected to be in the steady state and

$$[HOCO] = k_2[HCOOH]/k_7. \quad (8)$$

By solving the differential equations of

$$\frac{d[ClCOOH]}{dt} = k_2[Cl][HCOOH] - k_5[ClCOOH], \quad (9)$$

$$\frac{d[Cl]}{dt} = -2k_2[Cl][HCOOH], \quad (10)$$

we derived the concentration of ClCOOH as

$$[ClCOOH] = [Cl]_0 \frac{k_2[HCOOH]}{2k_2[HCOOH] - k_5} \times [\exp(-k_5 t) - \exp(-2k_2[HCOOH]t)]. \quad (11)$$

The temporal profile of the absorbance integrated over the 1350–1250 cm^{-1} region, including absorption of both *c*-ClCOOH and *t*-ClCOOH, upon photodissociation at 355 nm of a flowing mixture of $HCOOH/Cl_2/N_2$ (1/9/103 at 58 Torr) is shown in Fig. 6. When we fitted this profile to Eq. (11), we derived first-order rate coefficients as $k_2[HCOOH] = (2.7 \pm 0.7) \times 10^3$ s^{-1} and $k_5 = (9.2 \pm 2.7) \times 10^3$ s^{-1}, respectively. Using the initial concentrations of $[HCOOH] = 1.5 \times 10^{16}$ molecule cm^{-3} and assuming that reaction (2) is rate-determining for the formation of ClCOOH, we estimated a bimolecular reaction rate coefficient of $k_2 = (1.8 \pm 0.5) \times 10^{-13}$ at 363 K, consistent with the literature value of $\sim 2 \times 10^{-13}$ cm^3 $molecule^{-1}$ s^{-1} at 298 K.[9,10] The k_5 value at 363 K derived in this work is about one twentieth of the

value, 1.8×10^5 s^{-1}, derived from the rate equation reported by Jensen and Pimentel.[14] This also indicates that the 768 cm^{-1} band observed by them might not be due to ClCOOH.

VI. CONCLUSION

Four IR absorption bands of two conformers of ClCOOH were observed with a step-scan Fourier-transform spectrometer upon irradiation at 355 nm of a flowing gaseous mixture of Cl_2 and HCOOH in N_2. By considering possible chemical reactions, vibrational wavenumbers, rotational contours, relative IR intensities, and relative concentrations predicted with quantum-chemical calculations, we attributed absorption bands with origins at 1808.0 and 1328.5 cm^{-1} to the C=O stretching and COH bending modes of *t*-ClCOOH, respectively. Similarly, band origins at 1883.0 and 1284.9 cm^{-1} are assigned as the C=O stretching and COH bending modes of *c*-ClCOOH, respectively. From the observed and predicted relative intensities, we estimate that *t*-ClCOOH is more stable than *c*-ClCOOH by $\sim3\pm2$ kJ mol^{-1}, consistent with quantum-chemical calculations.

ACKNOWLEDGEMENTS

We thank J. S. Francisco for bringing to our attention the importance of ClCOOH. National Science Council of Taiwan (Grant No. NSC97-2113-M009-009-MY3) and the MOE-ATU project of National Chiao Tung University supported this work. We thank V. Stakhursky and T. A. Miller for providing the SpecView software for spectral simulation.

[1] J. Heicklen, *Atmospheric Chemistry* (Academic, New York, 1976).
[2] I. W. M. Smith and R. Zellner, J. Chem. Soc., Faraday Trans. 2 **69**, 1617 (1973).
[3] G. Paraskevopoulos and R. S. Irwin, J. Chem. Phys. **80**, 259 (1984).
[4] J. Warnatz, in *Combustion Chemistry*, edited by W. C. Gardiner, Jr. (Springer-Verlag, New York, 1984), p. 197.
[5] M. Legrand and M. De Angelis, J. Geophys. Res. **100**(D1), 1445 (1995).
[6] A. Galano, J. R. Alvarez-Idaboy, M. E. Ruiz-Santoya, and A. Viver-Bunge, J. Phys. Chem. A **106**, 9520 (2002) (and references therein).
[7] A. Miyoshi, H. Matsui, and N. Washida, J. Chem. Phys. **100**, 3532 (1994).
[8] H. L. West and G. K. Rollefson, J. Am. Chem. Soc. **58**, 2140 (1936).
[9] Q. Li, M. C. Osborne, and I. W. M. Smith, Int. J. Chem. Kinet. **32**, 85 (2000).
[10] T. J. Wallington, J. M. Andino, J. C. Ball, and S. M. Japar, J. Atmos. Chem. **10**, 301 (1990).
[11] G. S. Tyndall, T. J. Wallington, and A. R. Potts, Chem. Phys. Lett. **186**, 149 (1991).
[12] W. H. Hocking, Z. Naturforsch. A **31**, 1113 (1976).
[13] K. C. Herr and G. C. Pimentel, Appl. Opt. **4**, 25 (1965).
[14] R. J. Jensen and G. C. Pimentel, J. Phys. Chem. **71**, 1803 (1967).
[15] J. S. Francisco and W. A. Ghoul, Chem. Phys. **157**, 89 (1991).
[16] M. Remko, J. Mol. Struct.: THEOCHEM **492**, 203 (1999).
[17] E. H. Stephenson, B. Smyk, and J. N. Macdonald, J. Chem. Soc., Faraday Trans. **91**, 789 (1995).
[18] M. Gruber-Stadler, M. Mühlhäuser, and C. J. Nielsen, J. Phys. Chem. A **110**, 6157 (2006).
[19] H.-G. Yu, J. S. Francisco, and J. T. Muckerman, J. Chem. Phys. **129**, 064301 (2008).
[20] S.-H. Chen, L.-K. Chu, Y.-J. Chen, I-C. Chen, and Y.-P. Lee, Chem. Phys. Lett. **333**, 365 (2001).
[21] L.-K. Chu, Y.-P. Lee, and E. Y. Jiang, J. Chem. Phys. **120**, 3179 (2004).
[22] L.-K. Chu and Y.-P. Lee, J. Chem. Phys. **124**, 244301 (2006).
[23] L.-K. Chu and Y.-P. Lee, J. Chem. Phys. **126**, 134311 (2007).
[24] L.-K. Chu, H.-L. Han, and Y.-P. Lee, J. Chem. Phys. **126**, 174310 (2007).
[25] D.-R. Huang, L.-K. Chu, and Y.-P. Lee, J. Chem. Phys. **127**, 234318 (2007).
[26] W. Uhmann, A. Becker, C. Taran, and F. Siebert, Appl. Spectrosc. **45**, 390 (1991).
[27] A. D. H. Clague and H. J. Bernstein, Spectrochim. Acta, Part A **25**, 593 (1969).
[28] Y. Chen and L. Zhu, J. Phys. Chem. A **107**, 4643 (2003).
[29] M. J. Frisch, G. W. Trucks, H. B. Schlegel *et al.*, GAUSSIAN 03, Revision B.1 (Gaussian Inc., Pittsburgh, PA, 2003).
[30] A. D. Becke, J. Chem. Phys. **98**, 5648 (1993).
[31] C. Lee, W. Yang, and R. G. Parr, Phys. Rev. B **37**, 785 (1988).
[32] T. H. Dunning, Jr., J. Chem. Phys. **90**, 1007 (1989).
[33] D. E. Woon and T. H. Dunning, Jr., J. Chem. Phys. **98**, 1358 (1993).
[34] M. Freytes, D. Hurtmans, S. Kassi, J. Liévin, J. V. Auwera, A. Campargue, and M. Herman, Chem. Phys. **283**, 47 (2002).
[35] G. C. Schatz and J. Dyck, Chem. Phys. Lett. **188**, 11 (1992).
[36] M. Aoyagi and S. Kato, J. Chem. Phys. **88**, 6409 (1988).
[37] K. Kudla, G. C. Schatz, and A. F. Wagner, J. Chem. Phys. **95**, 1635 (1991).
[38] K. Kudla, A. G. Koures, L. B. Harding, and G. C. Schatz, J. Chem. Phys. **96**, 7465 (1992).
[39] D. C. Clary and G. C. Schatz, J. Chem. Phys. **99**, 4578 (1993).
[40] R. Valero and G.-J. Kroes, J. Chem. Phys. **117**, 8736 (2002).
[41] X. Song, J. Li, H. Hou, and B. Wang, J. Chem. Phys. **125**, 094301 (2006) (and references therein).
[42] Y. Li and J. S. Francisco, J. Chem. Phys. **113**, 7963 (2000).
[43] J. T. Petty and C. B. Moore, J. Mol. Spectrosc. **161**, 149 (1993).
[44] T. J. Sears, W. M. Fawzy, and P. M. Johnson, J. Chem. Phys. **97**, 3996 (1992).
[45] H. E. Radford, W. Wei, and T. J. Sears, J. Chem. Phys. **97**, 3989 (1992).
[46] D. E. Milligan and M. E. Jacox, J. Chem. Phys. **54**, 927 (1971).
[47] M. E. Jacox, J. Chem. Phys. **88**, 4598 (1988).
[48] D. Forney, M. E. Jacox, and W. E. Thompson, J. Chem. Phys. **119**, 10814 (2003).
[49] V. Stakhursky and T. A. Miller, 56th OSU International Symposium on Molecular Spectroscopy, Columbus, Ohio, 2001; SPECVIEW: Simulation and Fitting of Rotational Structure of Electronic and Vibronic Bands, http://www.chemistry.ohio-state.edu/~vstakhur.
[50] H.-T. Yu, Y.-J. Chi, H.-G. Fu, Z.-S. Li, and J.-Z. Sun, Chin. J. Chem. **21**, 244 (2003).